Ultrasonics - Sonochemistry 70 (2021) 105352

Contents lists available at ScienceDirect

Ultrasonics - Sonochemistry

journal homepage: www.elsevier.com/locate/ultson

Effect of multi-frequency ultrasound thawing on the structure and rheological properties of myofibrillar proteins from small yellow croaker

Yao-Yao Wang, Muhammad Tayyab Rashid, Jing-Kun Yan, Haile Ma*

School of Food & Biological Engineering, Institute of Food Physical Processing, Jiangsu University, Zhenjiang 212013, China

ARTICLE INFO

Keywords:
Larimichthys polyactis
Multi-frequency ultrasound
Thawing
Myofibrillar proteins
Protein structure
Rheological properties

ABSTRACT

The influence of multi-frequency combined ultrasound thawing on primary, secondary, and tertiary structures, electrophoresis pattern, particle size distribution, zeta potential values, thermal stability, rheological behavior, and microstructure of small yellow croaker myofibrillar proteins (MPs) were studied. Four treatments were used for thawing small yellow croakers: flow water thawing (FWT), mono-frequency ultrasonic thawing (MUT), dual-frequency ultrasonic thawing (DUT), and tri-frequency ultrasonic thawing (TUT). Compared with fresh samples (FS), the MPs of the sample pretreated by DUT had non-significant effect on protein primary (including free amino groups and surface hydrophobicity), secondary, tertiary structures, electrophoresis pattern, and microstructure. MPs pretreated by DUT had less aggregation and degradation. Besides, DUT treatment increased the thermal stability of MPs. The ultrasound had significant effects on the rheological properties of MPs. Overall, DUT effectively minimized the changes in MPs structure and protected the protein thermal stability and rheological behavior during the thawing process.

1. Introduction

Small yellow croaker (*Larimichthys polyactis*) is widely distributed in the Yellow, Bohai, and East China Seas [1]. This fish is very popular in customers because of high nutritional contents and deliciousness. Fresh fish meat is easy to spoil because it contains proteins, microorganisms, and enzymes, so it is often preserved by freezing on small and large scale. Therefore, the preservation of fish by different thawing ways to maintain the product quality has been a main concern of many researchers in recent years.

Recently, some new thawing methods have been developed to thaw meat products, such as high-voltage electrostatic field thawing [2], microwave thawing [3], and so on. Jia et al. revealed that high-voltage electrostatic field thawing prevents the oxidation of cysteine and methionine in myosin in pork [2]. Besides, Cao et al. [3] found that red seabream fillets thawed with magnetic nanoparticles plus microwave (MNPM) and magnetic nanoparticles plus far-infrared (MNPF) have good thermal stability and desirable gelling properties. However, there are still many shortcomings in them, such as oxidation of proteins and lipids, drip loss, and localized overheating. As one of the new thawing methods, ultrasonic thawing has been applied to thawed meat [4], fruits [5], and other products. Different from the traditional heat transfer method of thawing from outside to inside, the ultrasonic-assisted thawing process absorbs the heat generated by the ultrasonic attenuation both outside and inside of the food, to achieve the purpose of thawing and significantly improve the thawing efficiency [5]. However, only a few studies have been reported the effects of thawing methods on protein structure and properties of meat and meat products.

Myofibrillar proteins (MPs) are the most important functional component of muscle protein, which are salt-soluble protein, accounting for 55 to 60% of total muscle protein, and MPs are mainly composed of myosin, actin, tropomyosin, and a small number of regulatory structural proteins of unknown function [6]. The gel properties of MPs have important functional properties of fish meat and the determinants of the unique texture, water retention, and sensory properties of fish meat [7]. Few studies revealed that ultrasound thawing has a certain degree of influence on the structure, elasticity, stability and solubility of MPs [6–8]. Pulsed ultrasound had the potential to improve the gel properties of low-saturated fat meat products, and the chicken breast MPs treated by pulsed ultrasound had greater viscoelastic properties than the untreated samples [8]. Furthermore, Cai et al. [7] found that red seabream actin after ultrasound-assisted vacuum thawing had better thermal stability, regular secondary structure, and less tertiary structure unfold. Similarly, strong physical force generated by high-intensity ultrasound can destroy the structure of filamentous myosin, thereby effectively improving the solubility and dispersion

* Corresponding author.
E-mail address: mhl@ujs.edu.cn (H. Ma).

https://doi.org/10.1016/j.ultsonch.2020.105352
Received 2 August 2020; Received in revised form 7 September 2020; Accepted 13 September 2020
Available online 17 September 2020
1350-4177/

stability of MPs in water [6]. However, the research on the use of ultrasonic waves to thaw fish products is still in its infancy, and most of them still use mono-frequency ultrasonic waves for thawing. Thus, the research on the effect of multi-frequency ultrasonic thawing on the structure and rheological properties of food has not been reported yet.

Based on the above facts, the study aimed to analyze the changes in primary, secondary, and tertiary structures of MPs of small yellow croaker thawed by multi-frequency combined ultrasonic (including mono-, dual- and tri-frequency ultrasound). Furthermore, protein thermal stability, electrophoresis pattern, microstructure, particle size distribution, zeta potential values, and rheological behavior of MPs were also discussed.

2. Materials and methods

2.1. Sample preparation

Small yellow croaker was purchased from Lv Si Fishery (Jiangsu province, China) and transported back to the laboratory in a foam box containing crushed ice. The fish were procured, deceased, and harvested from mid- October to mid- November (used the same batch fish for each experiment). The linear probe of the thermometer was inserted into the back muscle of the fish and use it to detect the temperature at any time. The fish were quickly frozen in the −80 °C. When the thermometer showed that the temperature of the fish reached −18 °C, the fish were transferred to the freezer at −18 °C. After 48 h, the thawing test was conducted.

2.2. Thawing methods

2.2.1. Ultrasound thawing

The quick-frozen fish were thawed by multi-frequency ultrasonic equipment (Fig. 1). The samples were placed in an ultrasonic bath. The water temperature was controlled by a low-temperature cycle refrigerator to 10 °C ± 0.2, and the peristaltic pump controls the flow rate of water at 300 rpm. The ultrasonic power density was set to 50 W/L. Mono-frequency, dual-frequency, and triple-frequency ultrasonic were used to thawed fish, respectively. For mono-frequency ultrasonic thawing (MUT), the ultrasonic frequency was set to 20 kHz. For dual-frequency ultrasonic thawing (DUT), the combination of ultrasonic frequencies 20 and 40 kHz were used. For tri-frequency ultrasonic thawing (TUT), the combination of ultrasonic frequencies 20, 40 and 60 kHz were used. All the samples thawed by ultrasound were tested at each frequency for 5 s, each ultrasonic frequency was carried out alternately and orderly, then recycle back and forth in order.

2.2.2. Flow water thawing (FWT)

The flow rate of water was controlled by a peristaltic pump, set to 300 rpm, and the water temperature was set to 10 °C ± 0.2. The thawing cavity and the ultrasonic thawing cavity have the same size and shape.

During the entire ultrasound thawing and flow water thawing (FWT) test, the geometric center temperature of the sample was recorded by digital thermometers (UT325, Youlide Co., Ltd., Guangdong, China). When the samples center temperature reached −1 °C, the thawing was stopped, and the samples were taken out. The samples were then skinned and gutted and their meat was used for further analysis.

2.3. Preparation of myofibrillar proteins (MPs)

Refer to the methods of Lefever et al. [9] for the extraction of myofibrillar proteins (MPs). Buffer configuration: Buffer A was 20 mM phosphate buffer containing 100 mM NaCl, 1 mM EDTA, pH 7.0; Buffer B was 25 mM phosphate buffer containing 0.6 mM NaCl, pH 7.0. The fish were skinned and gutted and the meat was cut into small pieces. The minced meat was added to buffer A at a ratio of 1:10 (W/V), mixed evenly, homogenized by a homogenizer (IKA T18 Ultra Turrax Digital Homogenizer, Germany) at 13000 rpm for 5 min, stopped for 10 s every 20 s to avoid protein overheat transsexual (the whole process was carried out on crushed ice) and then centrifuged at 6000 rpm for 10 min at 4 °C to take the precipitate. Afterwards, the same volume of buffer A was added and the entire process was repeated twice. A certain amount of buffer B was added to the precipitate, and then filtered through 4 layers of gauze. Finally, the precipitate obtained after centrifugation at 5500 rpm for 15 min at 4 °C was the MP solution. The biuret method

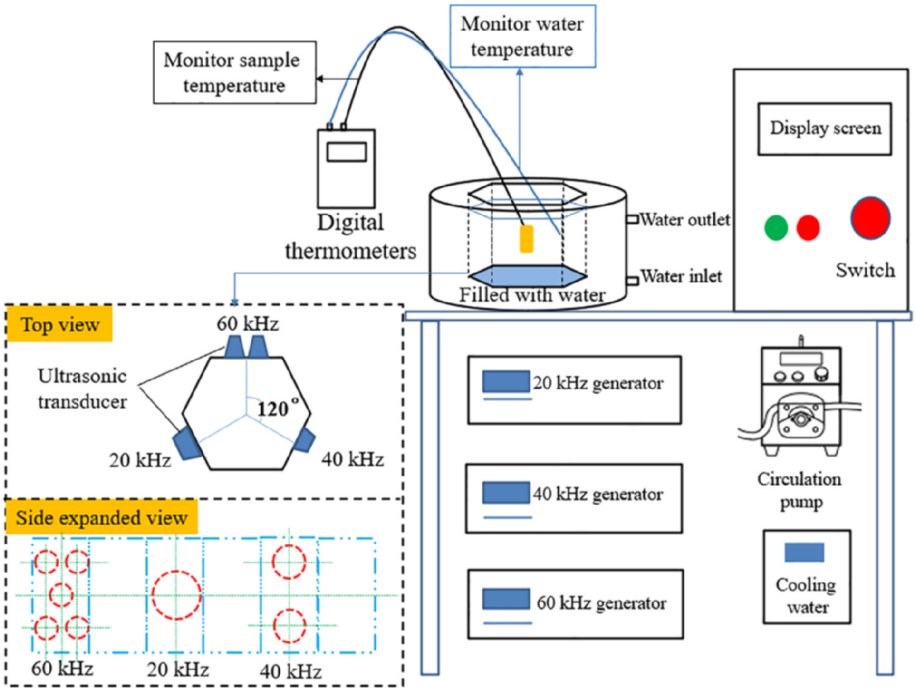

Fig. 1. Schematic diagrams of the multi-frequency ultrasound device.

was used to determine MP concentration [10].

2.4. MPs primary structure measurement

2.4.1. Surface hydrophobicity determination

The surface hydrophobicity of each MPs samples was measured according to You et al. [11] with a Cary Eclipse fluorescence spectrophotometer (Varian Inc., Palo Alto, USA). The excitation wavelength and the emission wavelength were set to 370 nm and 465 nm, respectively, and the slit width were both 2.5 nm. The scanning speed was 120 nm/min. The initial slope was calculated by linear regression analysis.

2.4.2. Free amino group determination

The content of free amino groups (NH_2) was determined according to the method of Adler- Nissen [12] with slight modification. The MP solution was diluted to 0.1 mg/mL with 0.20 M phosphate buffer (pH 8.2) containing 1% sodium lauryl sulfate. Then, 0.25 mL of MP solution was added to 2.0 mL of 0.10% 2,4,6-trinitrobenzene sulfonic acid (TNBS), and the reaction was carried out in a water bath at 50 °C for 1 h in the dark. 4.0 mL of HCl (0.1 M) was added to stop the reaction, and the mixture was allowed to stand at 25 °C for 30 min. The absorbance was measured at 340 nm using a spectrophotometer (Genesys 20, Thermo Fisher Scientific, Fair Lawn, NJ), and the content of free NH_2 (mmol/g protein) was determined by comparison with an L-leucine calibration curve.

2.5. Circular dichroism spectra measurement

The secondary structure of MPs was determined using a circular dichroism (CD) spectropolarimeter (Jasco J-715, Jasco Corp., Tokyo, Japan) with a scan rate of 50 nm/min. The quartz colorimetric optical path was 1.0 mm and the scanning wavelength was set to 195 nm to 250 nm [13].

2.6. Intrinsic fluorescence measurement

The fluorescence intensity of MP solution was measured according to the method of Cao and Xiong [14]. The MP solution was diluted to 0.2 mg/mL with phosphate buffer B. The fluorescence intensity was measured using a Cary Eclipse spectrophotometer (Varian Inc., Palo Alto, USA) with an excitation wavelength of 283 nm, and an emission spectrum of 300 to 400 nm was obtained using a scanning speed of 1000 nm/min. Both the excitation slit width and the emission slit width were set to 10 nm.

2.7. Sodium dodecyl sulfate–polyacrylamide gel electrophoresis (SDS-PAGE) measurement

The concentration of MP solution was diluted to 5 mg/mL, mixed with the SDS-PAGE sample buffer (containing 4% SDS, 20% glycerin, 0.005% bromophenol blue, 10% β-mercaptoethanol) at 1:1, and boiled in boiling water for 10 min to fully dissolve the protein. Then, a polyacrylamide gel with a 12% separation gel and 5% concentration gel was put on the electrophoresis equipment (Junyi-Dongfang Electrophoresis Equipment Co., Ltd., Beijing, China). The injection volume of Marker (5–245 kDa, Sangon Biotech Co., Ltd., Shanghai, China) was 5 μL. Coomassie brilliant blue R-250 was used for staining for 50 min. Then immerse the gel in a decolorizing solution (methanol: glacial acetic acid: deionized water = 4.5: 1.0: 4.5) to carry out decolorization until the base color of the gel was colorless.

2.8. Particle size distribution and zeta potential measurement

The Zetasizer Nano ZS90 instrument (Malvern Instruments Corp., Malvern, England) was used to determine the particle size distribution and zeta potential of the MPs (0.1 mg/mL), and the Zetasizer software included with the instrument was used to calculate the average particle size and zeta potential.

2.9. Differential scanning calorimetry (DSC) measurement

The internal thermal transition of the sample was measured by a differential scanning calorimeter (DSC 204, Netzsch, Germany). The heating temperature was set 25 to 95 °C, and the heating rate was set to 3 °C /min under a nitrogen atmosphere (20 mL/min) [3]. The thermal analysis chart estimates the enthalpy ($\triangle$H) and peak transition temperature (T_{max}) through the software (Proteus Analysis) provided with the instrument.

2.10. Rheological behavior measurement

All rheological tests were carried out with a Discovery HR-1 hybrid rheometer (TA Instruments, New Castle, USA).

2.10.1. Thermal gelation ability of MPs

1.5 mL of MP solution (10 mg/mL) was placed between two parallel plates (diameter 40 mm, gap 1 mm), and a dynamic temperature scan test was performed at a rate of 2 °C /min from 25 to 90 °C. The samples were measured at a frequency of 0.1 Hz with a maximum strain of 2% in the oscillation mode to obtain the storage modulus (G') and phase angle (tan δ).

2.10.2. Effects of heating on viscoelastic properties of MPs in frequency sweep

The samples were heated to 30, 50, and 70 °C, respectively, and placed on the parallel plates, and the measurements were started when the temperature of the samples reached 25 °C. The frequency sweep range was set to 0.1 to 100 rad/s. An amplitude strain of 20% was applied to ensure that all dynamic measurements were made in the linear viscoelastic range [15].

2.10.3. Flow properties of MPs

A parallel plate geometry with a diameter of 40 mm was selected for flow properties measurement. The samples were allowed to stand on parallel plates for 2 min. The temperature of measurements was 25 °C, the gap distance was set to 1 mm, and the shear viscosity was measured within the shear rate range of 1–1000 s^{-1}.

2.11. Scanning electron microscopy measurement

The MP solution (40 mg/mL) was freeze-dried and fixed into a copper stub, then coated with gold and observed using the scanning electron microscopy (SEM) (S-4800, Hitachi) with a magnification of 2000 [16].

2.12. Statistical analysis

All experiments were conducted in three replicates and the mean ± standard deviation (SD) was used. The results were analyzed by one-way ANOVA at the significance level of $p < 0.05$ using SPSS 13.0 software (IBM Corporation, NY, USA). The graphs were drawn by Origin Pro Software Version 8.5 (Origin Lab Corp., MA, USA).

3. Results and discussion

3.1. Changes in MPs structure

3.1.1. Primary structure

The surface hydrophobicity of MPs can indicate the exposure degree of hydrophobic groups within protein molecules. As the surface hydrophobic groups more exposed, the surface hydrophobicity increased,

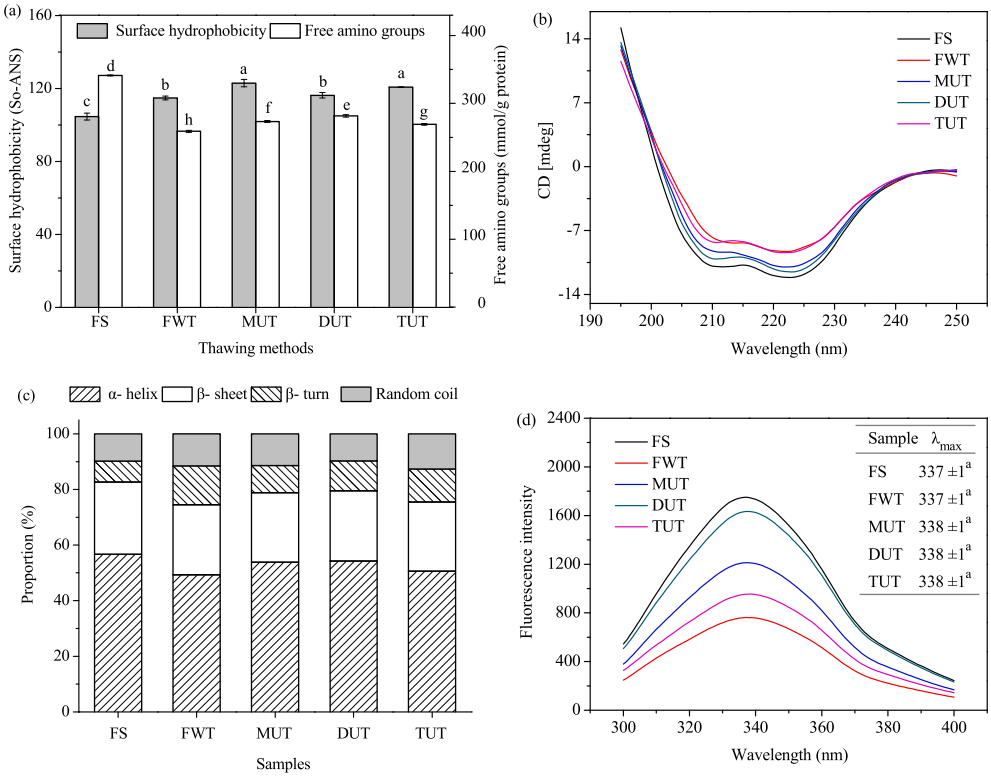

Fig. 2. Primary structure (a), circular dichroism spectra (b), different proportions of secondary structure (c), and intrinsic fluorescence (d) of MPs.

resulting in a greater degree of protein denaturation [17,18]. The effect of different thawing methods on the surface hydrophobicity of MPs were shown in Fig. 2 (a). Compared with FS, the surface hydrophobicity of MPs treated with FWT, MUT, DUT and TUT increased by 9.69, 17.48, 11.11 and 15.43%, respectively. It might be due to the hydrophobic regions of the exposed protein and thus increasing the surface hydrophobicity of the sample [19]. Zhang et al. [20] reported that before thawing, the hydrophobic amino acids of fresh MPs were embedded in the molecule, but the freezing and thawing processes exposed the hydrophobic groups of MPs and increased the hydrophobicity. Compared with FS, MUT, DUT, and TUT increased the hydrophobicity of MPs, the cavitation caused by ultrasonic waves may expand the protein chains folded on the surface of the protein, and the exposure of hydrophobic amino acids will lead to an increase in surface hydrophobicity [21]. During the thawing process, protein residues were exposed to water molecules, forming new hydrogen bonds, reducing the α-helix structure and increasing the surface hydrophobicity [22].

The changes of free amino content under different thawing conditions were shown in Fig. 2 (a). The free amino content of FS MPs was 341.26 μmol/mg. Compared with FS, FWT, MUT, DUT, and TUT decreased by 24.10, 19.89, 17.46, and 21.11%, respectively. Compared with the MPs obtained by MUT and TUT treatment, the MPs of the DUT treatment group had a higher free amino content, closest to the FS group. During the thawing process, the ε-NH_2 group converted to a carbonyl group by a deamination reaction, and these carbonyl derivatives then react with NH_2 groups, resulting in a further reduction in the free amino content [14]. Besides, Sun et al. [22] pointed out that lower ultrasonic power not caused the loss of free amino groups.

3.1.2. Secondary structure

It can be seen from Fig. 2 (b) and (c) that the secondary structure of MPs obtained by different treatments mostly exists in the form of α-helix. Compared with FS, the α-helix content of MPs treated with MUT, DUT, and TUT decreased to varying degrees, β-sheets increased in different proportions. It is because ultrasonic treatment changed the spatial entanglement of protein molecules, making their structure lose so that part of the protein was dissolved. The protein residues were exposed to water molecules, forming a new hydrogen bond, transforming the α-helix structure into a β-sheet structure [23,24]. Hu et al. [25] found that high-power ultrasonic treatment (400 W and 600 W) caused an increase in the α-helical structure of soybean protein isolate gel, while low-power treatment (200 W) caused a decrease in the α-helical structure. Compared with the MPs obtained by MUT and TUT treatment, the MPs of the DUT treatment group had a higher α-helix ratio, closest to the FS group. Sun et al. [26] reported that the decreased in the percentage of α-helical conformation and the increased in the content of random coils and β-sheets may be due to protein oxidation. The α-helix content had a negative linear relationship with the surface hydrophobicity. Therefore, the destruction of the α-helical structure was accompanied by an increase in surface hydrophobicity. This was consistent with the results of surface hydrophobicity studies (Fig. 2a). Huang et al. [24] pointed out that the secondary structure of the protein was connected with various types of hydrogen bonds. Ultrasonic treatment destroyed some hydrogen bonds and cause the ordered structure to change to the disordered structure, which was consistent with the results of this study.

3.1.3. Tertiary structure

Fluorescence spectra reflects the tertiary structure information of proteins. The fluorescence intensity usually comes from tryptophan, phenylalanine, and tyrosine residues [13,14]. The fluorescence spectrum of MPs thawed by different thawing methods were shown in Fig. 2 (d). It can be seen that the fluorescence intensity of MPs treated by FWT, MUT, DUT, and TUT was lower than that of FS. This may be due to the unfolding of the MPs during quick freezing and thawing [20]. Besides, protein aggregation and folding, as well as the oxidation of tryptophan, also reduce the fluorescence intensity. Sun et al. [22] studied the effect of different power ultrasonic freezing common carp on the tertiary structure of the myofibrillar proteins and found that after freezing treatment, the fluorescence intensity of all frozen groups was

lower than that of the fresh control group. The degree of protein conformation change reflected by the degree of maximum fluorescence emission peak (λmax) [14]. Zhang et al. [20] studied the effect of freeze–thaw cycles on the muscle structure of the porcine longissimus muscle and pointed out that as the number of freeze–thaw cycles increased, the fluorescence intensity gradually decreased, which may be caused by the unfolding of the protein during the freezing and thawing process. Compared with FS, the MPs processed by MUT, DUT and TUT showed redshift, but there was no significant difference ($p > 0.05$). Cai et al. [7] used the ultrasonic-assisted microwave, ultrasonic-assisted far-infrared and far-infrared to defrost red snapper fillets, and found that the samples thawed by these three methods had lower fluorescence intensity than the fresh group, and all had red migration phenomenon but no significant difference, which was consistent with the results of the current study.

3.2. MPs aggregation and degradation

MPs aggregation and degradation can reflect the changes in protein conformation [3], and they were indicated using SDS-PAGE, particle size and zeta potential. The change of electrophoretic bands can be used to reflect the aggregation, cross-linking of MPs or the change of intermolecular chemical bond [4]. The increase in particle size can reflect the formation of aggregates, or the destruction of hydrogen bonds in the protein structure. The higher the zeta potential, the stronger the structural stability of MPs [3].

3.2.1. SDS-PAGE

The SDS-PAGE of MPs pretreated by different methods was shown in Fig. 3 (a). Myosin heavy chain (MHC) and actin chain (AC) are the main bands. Density analysis of myosin heavy chain (Fig. 3b) found that the density of MP bands treated by FWT was low, which indicated that myosin had been degraded to some extent. The density of MPs bands treated by DUT was closest to the FS group, which indicated that there were less aggregation and degradation in the DUT samples. Also, there were no new bands and no old bands disappear. Similarly, Sun et al. [22] revealed that the ultrasound-assisted freezing affected the protein structure of carp at different power levels. It was found that ultrasound may cause protein conformational changes, but SDS-PAGE between fresh and frozen samples did not show obvious change. However, Cai

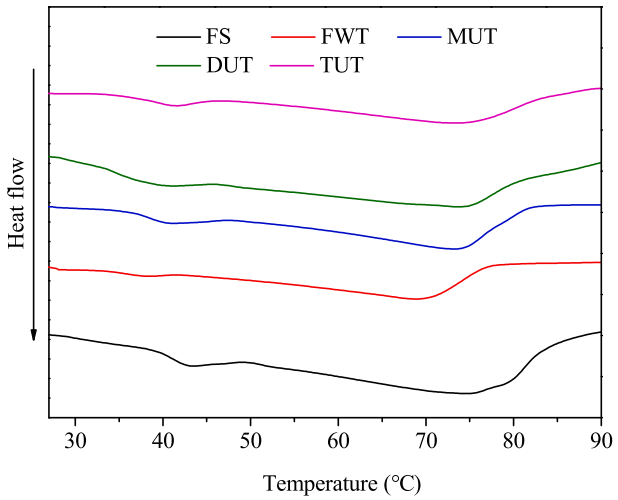

Fig. 4. Effect of different thawing treatments on differential scanning calorimetry (DSC) measurement of MPs.

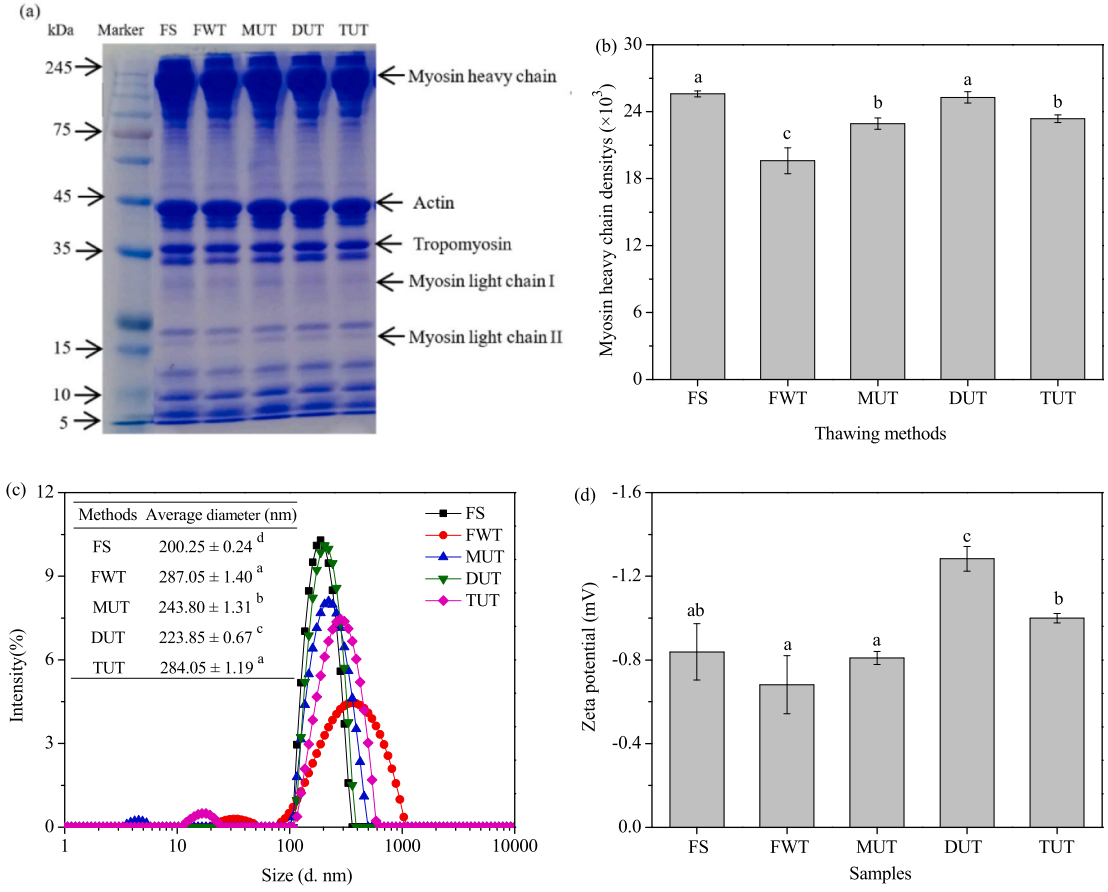

Fig. 3. The SDS-PAGE diagram (a), density in myosin heavy chain (b), intensity distributions of particle sizes (c) and zeta potentials (d) of MPs.

Table 1
Changes in the maximum transition temperature (T_{max}) and denaturation enthalpy (ΔH) of myosin (peak I) and actin (peak II) of MPs.

Treatment	Peak 1		Peak 2	
	$T_{max}1$ (°C)	ΔH_1 ($J \cdot g^{-1}$)	$T_{max}2$ (°C)	ΔH_2 ($J \cdot g^{-1}$)
FS	43.63 ± 0.09 [a]	0.28 ± 0.01 [a]	74.71 ± 0.33 [a]	1.59 ± 0.01 [a]
FWT	38.35 ± 0.03 [d]	0.21 ± 0.02[c]	68.53 ± 0.16[c]	1.48 ± 0.06[c]
MUT	39.48 ± 0.10[c]	0.24 ± 0.01[b]	71.41 ± 0.14[b]	1.53 ± 0.01 [bc]
DUT	40.99 ± 0.69[b]	0.25 ± 0.01[b]	74.47 ± 0.21 [a]	1.57 ± 0.01 [ab]
TUT	39.73 ± 0.33[c]	0.24 ± 0.01[b]	71.45 ± 0.09[b]	1.54 ± 0.02 [ab]

Values are means ± standard deviation. "a–d" letters indicated significant differences in the columns ($p < 0.05$).

et al. [4] compared fresh *Sciaenops ocellatus*, the MHC density of the ultrasonically thawed samples was lower, which indicates that myosin had been degraded to some extent. Ultrasound combined with microwave thawing was similar to fresh samples, which indicated that ultrasound combined with microwave thawing had less aggregation and degradation.

3.2.2. MPs aggregation

As can be seen from Fig. 3 (c), compared with FS, the average particle size of MPs treated with FWT, MUT, DUT, and TUT increased by 43.35, 21.75, 11.79, and 41.85% respectively. Oxidation and denaturation of MPs may cause the formation of aggregates during processing and storage, increasing in average particle size [14]. Compared with FWT, the size of samples treated by MUT, DUT, and TUT were smaller, and the average particle size of sample treated by DUT was the smallest. It can be concluded that DUT can reduce the aggregation of MPs and protect its structure. This may be due to the cavitation of ultrasonic waves causing the aggregates to be broken, thereby reducing the average particle size [25]. Li et al. [19] used different thawing methods to defrost the porcine longissimus muscle and studied the effect of different thawing methods on the average particle size of MPs in the porcine longissimus muscle. The results showed that compared with the fresh group, the average particle size values of microwave thawing, ultrasonic thawing (UT, 20 °C, 500 W, 45 min), vacuum thawing, water immersion thawing, and refrigeration thawing increased by 20.5, 0.9, 7.4, 13.2 and 9.4%, respectively, and pointed out that compared with the fresh group, the average particle size of MPs after ultrasonic thawing was not significant ($p > 0.05$), which may be related to the turbulence and shear force related high physical force.

In general, a higher zeta potential means that there is a larger distance between adjacent suspended particles in the sample solution and a larger electrostatic repulsion force [27]. It can be seen from Fig. 3 (d), that compared with MPs obtained by FWT treatment, MUT, DUT, and TUT treatments were significantly improved ($p < 0.05$). This may be because ultrasonic treatment exposed some polar groups inside the protein to the surface, resulting in a higher net charge of the MPs suspension [28]. Among them, the MPs processed by the DUT had the largest potential value. This showed that the MPs treated by DUT had the most uniform particle size distribution, and the MPs particles had the largest electrostatic repulsive force, thereby preventing the aggregation of proteins and having better stability. Arredondo-Parada et al. [29] pointed out that ultrasound-induced changes in protein surface charge are related to the expansion of protein conformation and the exposure of hydrophobic non-polar residues.

3.3. DSC

The DSC results of small yellow croaker MPs were shown in Fig. 4. It can be seen that there were two major endothermic peaks. The first peak was the thermal denaturation absorption peak of myosin, and the second peak was the thermal denaturation absorption peak of actin [30]. The maximum transition temperature (T_{max}) and enthalpy value ΔH of the two peaks were shown in Table 1. The $T_{max}1$ of FS was 43.63 °C, while the $T_{max}1$ of MPs treated with FWT, MUT, DUT, and TUT were 38.35, 39.48, 40.99, and 39.73 °C, respectively. It can be seen that the $T_{max}1$ of the sample treated by DUT was closest to the $T_{max}1$ of the FS. Besides, the $T_{max}2$ of FS was 74.71 °C, while the $T_{max}2$ of samples treated with FWT, MUT, DUT, and TUT were 68.53, 71.41, 74.47 and 71.45 °C, respectively. It can be seen that the $T_{max}2$ of the sample treated with DUT was closest to the $T_{max}2$ of the FS. Thence, the DUT-treated samples have higher thermal stability than FWT, MUT, and TUT samples. The significant decrease in the transition temperature indicates that the thermal stability of muscle protein was reduced during the thawing process [31]. Similarly, the ΔH_1 and ΔH_2 of myosin and actin of samples treated with FWT, MUT, DUT, and TUT were reduced, but the ΔH values of samples treated by DUT were higher than those of FWT, MUT and TUT treated samples. Similar to us, Sun et al. [30] found two endothermic peaks in carp muscles frozen with ultrasound-assisted immersion freezing, indicating that the weakening of hydrogen bonds and the increase of protein aggregation may lead to the decrease of △H and the destruction of protein structure. Overall, DUT might lead to less protein structure destruction and protein denaturation.

3.4. Rheological behavior

3.4.1. Thermal gelling ability of MPs

The effect of different thawing methods on the storage modulus (G') and phase angle (tan δ) of MPs at 25 to 90 °C were shown in Fig. 5 (a) and (b). G' was used to evaluate the energy storage due to elastic changes, and the tan δ was used to evaluate the viscoelastic properties in a single deflection cycle [32]. It can be seen from Fig. 5(a) G' represents the elastic component, initially rose slowly from 25 to 30 °C. The reason for the increase in storage modulus may be the agglomeration of myosin heads. This was the beginning of the gel process [33]. The G' value rises rapidly from 30 to 41 °C, and a peak appears at 41 °C. In the temperature range of 41 to 47 °C, the temperature drops significantly ($p > 0.05$). At this time, the non-covalent bond was broken, and the myosin tail was cross-linked. On one hand, it may be due to changes in the three-dimensional structure, on the other hand, it may be caused by the pressure caused by the movement of molecules and chemical bonds [15]. The G' value of the peak point of the MPs after MUT, DUT, and TUT treatment increased significantly relative to FWT, which may be due to the force applied by the ultrasonic wave to make the chain open better, thereby improving the formation of the connection area [34]. The G' value increased from 47 to 69 °C, and the network changed from viscous sol to elastic gel. This may be due to the formation of disulfide and hydrophobic bonds in the structure of myosin and actin, and the interaction formed was irreversible [34]. Compared with FWT, the G' value of the ultrasonically treated samples at this stage was higher than that of FS. As confirmed by the particle size distribution results (Fig. 3 c), the particle size becomes smaller and uniform under the effect of ultrasonic treatment. These smaller chains have better alignment and the possibility of forming irreversible bonds increases. Compared with the FS at 41 °C (6.46 Pa) and 69 °C (17.72 Pa), the G' value of MPs after FWT, MUT, DUT, and TUT

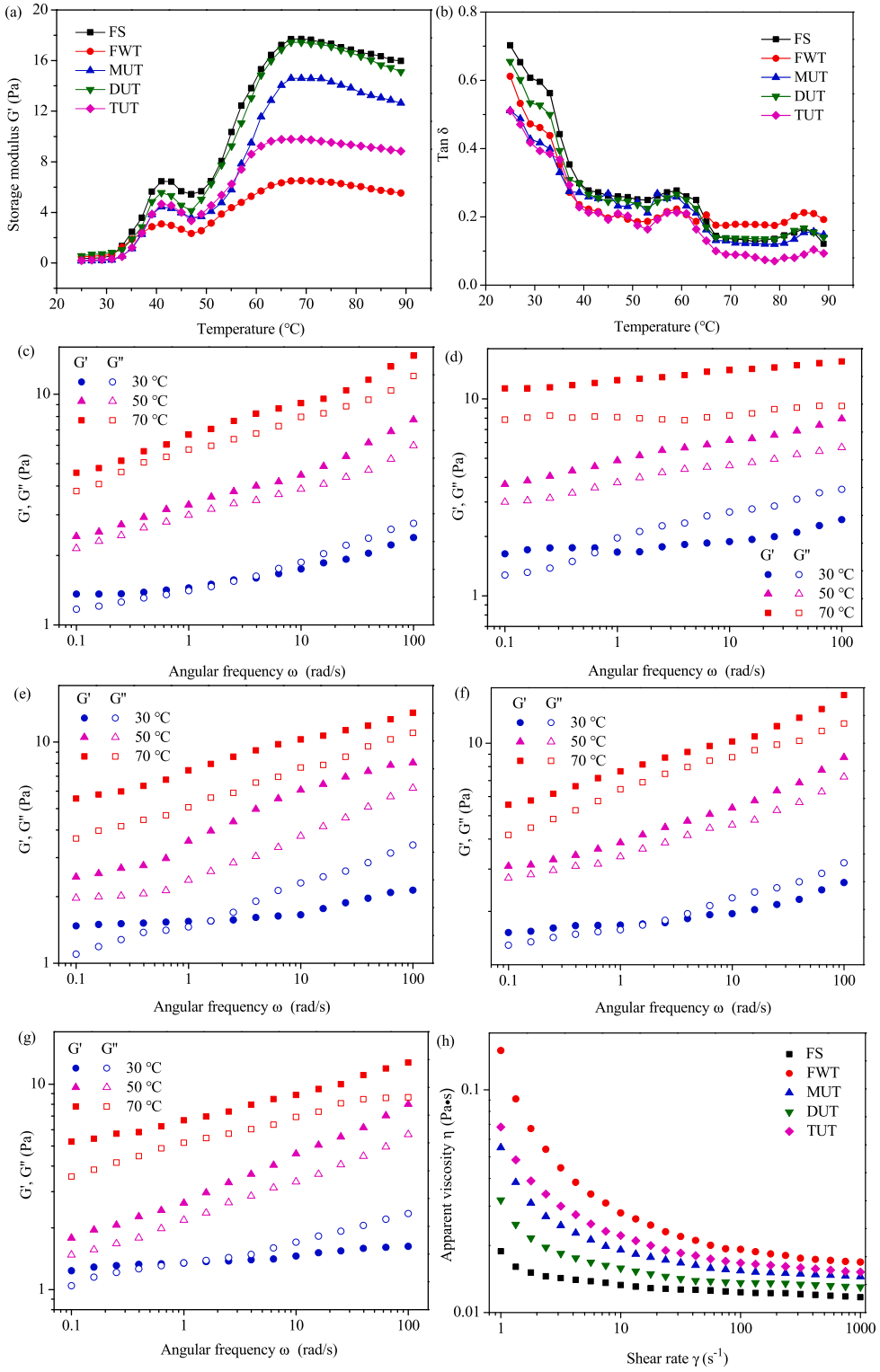

Fig. 5. Dynamic rheological properties: Changes in (a) storage modulus G' and (b) phase angle tan δ of different thawing treatments; Plots of storage modulus G' and loss modulus G" as a function of angular frequency ω for MPs ((c) FS, (d) FWT, (e) MUT, (f) DUT and (g) TUT) at 25 °C after different heating temperature treatments (30, 50 and 70 °C); (h) Flow curve of MPs (at 25 °C).

treatments decreased to varying degrees, but the MPs treated by DUT was closest to the FS. This shows that MPs from the DUT treatment formed a more elastic gel in most temperature regions.

The phase angle was used to evaluate the rheological behavior and viscoelasticity of the myofibrillar protein suspension, which is equal to the tangent of the G" value and the G' value [15]. As shown in the Fig. 5(b), the phase angle of all samples decreased during the heating process. The decrease in phase angle during heating indicates the difference between gel network structures.

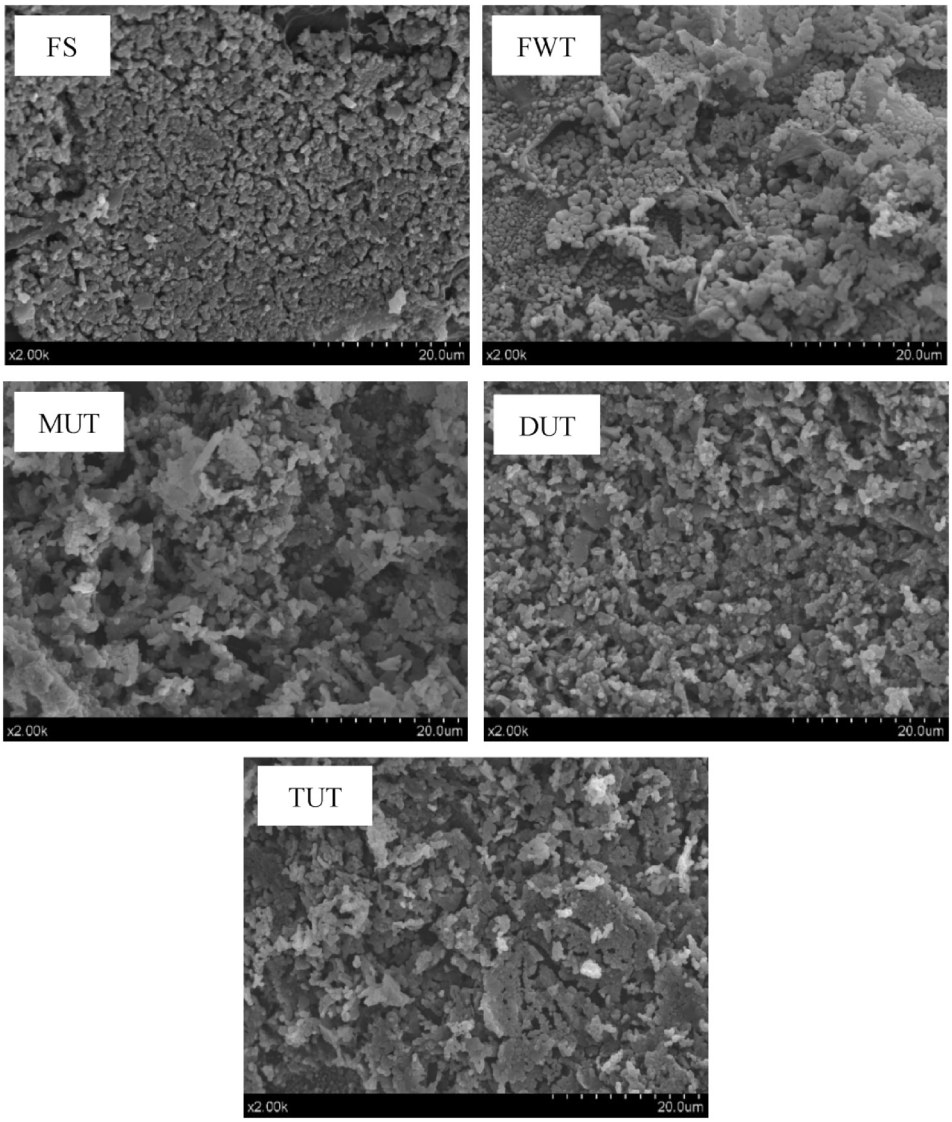

Fig. 6. Influence of different thawing methods on the microstructure of small yellow croaker MPs.

3.4.2. Effects of heating on viscoelastic properties of MPs in the frequency sweep

Fig. 5 (c)-(g) shows the relationship between angular frequency ω and G', G" values of MPs after FS, FWT, MUT, DUT, and TUT treatments when heated to various temperatures (30, 50 and 70 ˚C). The angular rate ranged from 0.1 to 100 rad/s. After heat treatment at 30 ˚C, each sample appeared as an elastic fluid in the low-frequency region and as a viscous fluid in the high-frequency region. In the relatively low-frequency range, due to the long deformation interval, the protein was prone to a large amount of entanglement behavior, and the elastic part (G') was the main response to vibration. At a relatively high frequency, the entanglement coupling of myofibrillar protein dominates and becomes a knot because the oscillation period was too short to unravel the molecular association [35,36]. When the temperature reached 50 ˚C, it results the G' higher than G" in the entire frequency range. As the temperature increased, the ability of MPs in different treatment groups to form temporary associations increased, so their rheological behavior may be an elastic dispersion. Besides, it can be predicted that the sol–gel transition temperature of each group samples was between 30 and 50 ˚C, which was consistent with the above results (Fig. 5 a). When the temperature was further increased to 70 ˚C, the G' value of MPs treated with FS, MUT, DUT, and TUT was significantly greater than G", and the two curves were almost parallel, indicating that there may still be mild protein aggregation during heating, this leads to the establishment of a weak gel system.

3.4.3. Flow properties of MPs

As shown in Fig. 5 (h), when the shear rate γ was low, the viscosity of all samples gradually decreased as the shear rate increased, showing shear thinning behavior, which appears as a non-Newtonian pseudoplastic fluid. This was probably because the increasing shear force causes the unwinding speed of the myofibrillar protein molecular chain to be faster than the winding speed, and the cross-linked structure was destroyed [15]. When the shear rate γ was high, the apparent viscosity of the sample solution was unchanged, showing Newtonian fluid behavior, it might be due to the shear force breaks most of the intermolecular entanglement [37]. At the same shear rate γ, the sample of the FS group has the lowest apparent viscosity η, and when the samples were subjected to quick freezing and thawing treatment, the apparent viscosity (η) increased. Compared with the sample treated with FWT, the η of MPs treated with MUT, DUT, and TUT decreased, which may be due to the decrease in molecular weight of MPs and the decrease in particle size under the action of ultrasound [38,39]. Among them, the viscosity of sample treated by DUT was closest to the FS group which was consistent with the results of particle size determination. Chen et al. [15] pointed out that myosin had a characteristic rod-like chain

structure and can be oriented under shearing. At low shear rates, rod-shaped molecules in MPs tend to overlap and fold, and the friction in the protein chain may cause it to have a higher viscosity. When the shear rate was increased, the connection between the myosin molecular chains was broken, thereby weakening the friction resistance and making the suspension easier to flow.

3.5. SEM

The microstructure of lyophilized MPs can be observed by SEM (Fig. 6). The sample surface of the FS group was relatively flat, the particles were small, and the arrangement was neat. The sample surface treated by the FWT had an irregular microstructure and there was aggregation. Compared with FS, the surface of sample treated by DUT was smoother and more uniform, and there was almost no aggregation of the sample. This was consistent with the results of particle size studies (Fig. 3 c). The change of MPs morphology obtained after ultrasonic thawing may be caused by the cavitation effect of ultrasonic waves during the thawing process, may lead to a large number of protein molecules to unfold and cause the internal hydrophobic groups to leak. Li et al. [19] used ultrasound (500 W, 20 ˚C, 45 min) to thaw (UT) the porcine longissimus muscle, and studied the effect of different thawing methods on the structure of myofibrillar protein gel. It was found that UT had the smallest effect on the microstructure of the MPs gel and was closest to the fresh control group. This may be due to the particle size of the MPs treated with UT was smaller, which was more conducive to the formation of microstructures characterized by smaller protein spacing, which was consistent with the results of particle size studies.

4. Conclusions

FWT, MUT, DUT, and TUT had different effects on the MPs of quick-frozen small yellow croakers. The MPs primary structure treated with DUT was closest to the FS group through the surface hydrophobicity and free amino groups. The MPs secondary and tertiary structures treated using DUT were more stable according to the CD spectrum and fluorescence spectra. There were no obvious changes in the SDS-PAGE patterns between the FS and thawed samples. Besides, the DUT had lower MPs aggregation according to particle size. DUT enhanced the stability of MPs according to the value of zeta potential. The DUT effectively maintains the thermal stability of the MPs. Ultrasonic thawing affects the rheological properties of MPs, the apparent viscosity of MPs after DUT was closest to the FS group. SEM analysis showed that the MPs treated by DUT has a regular structure and less aggregation. Thus, DUT can effectively reduce protein structure changes and protected the thermal stability and rheological properties of MPs.

CRediT authorship contribution statement

Yao-Yao Wang: Investigation, Methodology, Data curation, Formal analysis, Validation, Writing - original draft. **Muhammad Tayyab Rashid:** Visualization, Writing - review & editing. **Jing-Kun Yan:** Methodology, Software. **Haile Ma:** Conceptualization, Supervision, Project administration, Funding acquisition.

Declaration of Competing Interest

The authors declare that they have no known competing financial interests or personal relationships that could have appeared to influence the work reported in this paper.

Acknowledgment

This work was supported financially by the Key Research & Development Program (Modern Agriculture) of Jiangsu Province (BE2018368).

Appendix A. Supplementary data

Supplementary data to this article can be found online at https://doi.org/10.1016/j.ultsonch.2020.105352.

References

[1] J.S. Ren, X. Jin, T. Yang, S.A.L.M. Kooijman, X. Shan, A dynamic energy budget model for small yellow croaker larimichthys polyactis: Parameterisation and application in its main geographic distribution waters, Ecol. Model. 427 (2020) 109051.
[2] G.L. Jia, K. Sha, X.D. Feng, H.J. Liu, Post-thawing metabolite profile and amino acid oxidation of thawed pork tenderloin by HVEF-A short communication, Food Chem. 291 (2019) 16–21.
[3] M.J. Cao, A.L. Cao, J. Wang, L.Y. Cai, J. Regenstein, Y.J. Ruan, X.X. Li, Effect of magnetic nanoparticles plus microwave or far-infrared thawing on protein conformation changes and moisture migration of red seabream (*Pagrus major*) fillets, Food Chem. 266 (2018) 498–507.
[4] L. Cai, W. Zhang, A. Cao, M. Cao, J. Li, Effects of ultrasonics combined with far infrared or microwave thawing on protein denaturation and moisture migration of *Sciaenops ocellatus* (red drum), Ultrason. Sonochem. 55 (2019) 96–104.
[5] Y. Liu, S.H. Chen, Y.F. Pu, A.I. Muhammad, M.J. Hang, D.H. Liu, T. Ye, Ultrasound-assisted thawing of mango pulp: Effect on thawing rate, sensory, and nutritional properties, Food Chem. 286 (2019) 576–583.
[6] H. Liu, H. Zhang, Q. Liu, Q. Chen, B.H. Kong, Solubilization and stable dispersion of myofibrillar proteins in water through the destruction and inhibition of the assembly of filaments using high-intensity ultrasound, Ultrason. Sonochem. 67 (2020) 105160.
[7] L. Cai, M. Cao, A. Cao, J. Regenstein, J. Li, R. Guan, Ultrasound or microwave vacuum thawing of red seabream (*Pagrus major*) fillets, Ultrason. Sonochem 47 (2018) 122–132.
[8] Y.Y. Zhao, P. Wang, Y.F. Zou, K. Li, Z.L. Kang, X.L. Xu, G.H. Zhou, Effect of pre-emulsification of plant lipid treated by pulsed ultrasound on the functional properties of chicken breast myofibrillar protein composite gel, Food Res. Int. 58 (2014) 98–104.
[9] F. Lefever, B. Fauconneau, J.W. Thompson, T.A. Gill, Thermal denaturation and aggregation properties of atlantic salmon myofibrils and myosin from white and red muscles, J. Agr. Food Chem 55 (12) (2007) 4761–4770.
[10] A.G. Gornall, C.J. Bardawill, M.M. David, Determination of serum proteins by means of the biuret reaction, J. Biol. Chem. 171 (1949) 751–766.
[11] J. You, J. Pan, H. Shen, Y. Luo, Changes in physicochemical properties of bighead carp (*Aristichthys mobilis*) actomyosin by thermal treatment, Int. J. Food Prop. 15 (6) (2012) 1276–1285.
[12] J. Adler-Nissen, Determination of the degree of hydrolysis of food protein hydrolysates by trinitrobenzene sulfonic acid, J. Agr Food Chem. 27 (6) (1979) 1256–1262.
[13] Q. Liu, Y. Lu, J.C. Han, Q. Chen, B.H. Kong, Structure-modification by moderate oxidation in hydroxyl radical-generating systems promote the emulsifying properties of soy protein isolate, Food Struct. 6 (10) (2015) 21–28.
[14] Y. Cao, Y.L. Xiong, Chlorogenic acid-mediated gel formation of oxidatively stressed myofibrillar protein, Food Chem. 180 (2015) 235–243.
[15] X. Chen, X. Xu, D. Liu, G. Zhou, M. Han, P. Wang, Rheological behavior, conformational changes and interactions of water-soluble myofibrillar protein during heating, Food Hydrocolloids 77 (2018) 524–533.
[16] J.Y. Wang, Y.L. Yang, X.Z. Tang, W.X. Ni, L. Zhou, Effects of pulsed ultrasound on rheological and structural properties of chicken myofibrillar protein, Ultrason. Sonochem. 38 (2017) 225–233.
[17] G. Jia, S. Nirasawa, X. Ji, Y. Luo, H. Liu, Physicochemical changes in myofibrillar proteins extracted from pork tenderloin thawed by a high-voltage electrostatic field, Food Chem. 240 (1) (2017) 910–916.
[18] G. Jia, H. Liu, S. Nirasawa, H. Liu, Effects of high-voltage electrostatic field treatment on the thawing rate and post-thawing quality of frozen rabbit meat, Innov. Food Sci. Emerg. 41 (6) (2017) 348–356.
[19] F.F. Li, B. Wang, Q. Liu, Q. Chen, H.W. Zhang, X.F. Xia, B.H. Kong, Changes in myofibrillar protein gel quality of porcine longissimus muscle induced by its structural modification under different thawing methods, Meat Sci. 147 (2019) 108–115.
[20] M.C. Zhang, F.F. Li, X.P. Diao, B.H. Kong, X.F. Xia, Moisture migration, microstructure damage and protein structure changes in porcine longissimus muscle as influenced by multiple freeze-thaw cycles, Meat Sci. 133 (11) (2017) 10–18.
[21] Z. Zhang, J.M. Regenstein, P. Zhou, Y. Yang, Effects of high intensity ultrasound modification on physicochemical property and water in myofibrillar protein gel, Ultrason. Sonochem. 34 (1) (2017) 960–967.
[22] Q.X. Sun, Q. Chen, X.F. Xia, B.H. Kong, X.P. Diao, Effects of ultrasound-assisted freezing at different power levels on the structure and thermal stability of common carp (*Cyprinus carpio*) proteins, Ultrason. Sonochem. 54 (2019) 311–320.
[23] X.X. Zhou, H. Chen, F. Lyu, H.H. Lin, Q. Zhang, Y.T. Ding, Physicochemical properties and microstructure of fish myofibrillar protein lipid composite gels: Effects of fat type and concentration, Food Hydrocolloids 90 (2019) 433–442.
[24] L.R. Huang, X.N. Ding, Y.L. Li, H.L. Ma, The aggregation, structures and emulsifying properties of soybean protein isolate induced by ultrasound and acid, Food Chem. 279 (2019) 114–119.

[25] H. Hu, L.C. Ecy, L. Wan, M. Tian, S. Pan, The effect of high intensity ultrasonic pretreatment on the properties of soybean protein isolate gel induced by calcium sulfate, Food Hydrocolloids 32 (2) (2013) 303–311.
[26] W. Sun, F. Zhou, D.W. Sun, M. Zhao, Effect of oxidation on the emulsifying properties of MPs, Food Bioprocess Tech. 6 (2013) 1703–1712.
[27] P.P. Esteban, A.T.A. Jenkins, T.C. Arnot, Elucidation of the mechanisms of action of Bacteriophage K/nano-emulsion formulations against S. aureus via measurement of particle size and zeta potential, Colloid. Surface. B. 139 (2016) 87–94.
[28] X. Shi, H. Zou, S. Sun, Z. Lu, T. Zhang, J. Gao, C. Yu, Application of high-pressure homogenization for improving the physicochemical, functional and rheological properties of myofibrillar protein, Int. J. Biol. Macromol. 138 (2019) 425–432.
[29] I. Arredondo-Parada, W. Torres-Arreola, G.M. Suárez-Jiménez, J.C. Ramírez Suárez, J.E. Juárez-Onofre, F. Rodríguez-Félix, E. Marquez-Rios, Effect of ultrasound on physicochemical and foaming properties of a protein concentrate from giant squid (*Dosidicus gigas*) mantle, LWT-Food, Sci. Technol. 121 (2020) 108954.
[30] Q. Sun, F. Sun, X. Xia, H. Xu, B. Kong, The comparison of ultrasound-assisted immersion freezing, air freezing and immersion freezing on the muscle quality and physicochemical properties of common carp (Cyprinus carpio) during freezing storage, Ultrason. Sonochem. 51 (2019) 281–291.
[31] L. Huang, Q. Liu, X.F. Xia, B.H. Kong, Y.L. Xiong, Oxidative changes and weakened gelling ability of salt-extracted protein are responsible for textural losses in dumpling meat fillings during frozen storage, Food Chem. 185 (2015) 459–469.
[32] A. Amir, M. Shahedi, Kadivar. Structural properties of gluten modified by ascorbic acid and transglutaminase, Int. J. Food Pro. 20 (2017) 1588-1599.
[33] J. Jiang, Y.L. Xiong, Extreme pH treatments enhance the structure reinforcement role of soy protein isolate and its emulsions in pork myofibrillar protein gels in the presence of microbial transglutaminase, Meat Sci. 93 (3) (2013) 469–476.
[34] K. Li, Z.L. Kang, Y.Y. Zhao, X.L. Xu, G.H. Zhou, Use of high-intensity ultrasound to improve functional properties of batter suspensions prepared from PSE-like chicken breast meat, Food Bioprocess Tech. 7 (12) (2014) 3466–3477.
[35] J.K. Yan, W.D. Cai, C. Wang, Y.B. Yu, H.N. Zhang, Y. Yang, et al., Macromolecular behavior, structural characteristics and rheological properties of alkali-neutralization curdlan at different concentrations, Food Hydrocolloids 105 (2020) 105787.
[36] Y. Zhang, X. Xu, J. Xu, L. Zhang, Dynamic viscoelastic behavior of triple helical Lentinan in water: Effects of concentration and molecular weight, Polymer 48 (22) (2007) 6681–6690.
[37] W.D. Cai, J. Zhu, L.X. Wu, Z.R. Qiao, L. Li, J.K. Yan, Preparation, characterization, rheological and antioxidant properties of ferulic acid-grafted curdlan conjugates, Food Chem. 300 (2019) 125221.
[38] W.Y. Qiu, W.D. Cai, M. Wang, J.K. Yan, Effect of ultrasonic intensity on the conformational changes in citrus pectin under ultrasonic processing, Food Chem. 297 (2019) 125021.
[39] R.M. Aadil, X.A. Zeng, Z. Han, D.W. Sun, Effects of ultrasound treatments on quality of grapefruit juice, Food Chem. 141 (3) (2013) 3201–3206.